1-1-2011

Thermal stability of infrared stimulated luminescence of sedimentary K-feldspar

Bo Li
University of Hong Kong, bli@uow.edu.au

Sheng-Hua Li
University of Hong Kong

Thermal stability of infrared stimulated luminescence of sedimentary K-feldspar

Abstract

The thermal stability of the infrared stimulated luminescence (IRSL) signal measured at 50 °C as a function of IR stimulation time was investigated using KF grains extracted from sediments from central China. A dependence of thermal stability of IRSL signal on IR stimulation time and stimulation temperature were observed in pulse annealing studies. Relatively lower thermal stability is given by the initial part of the IRSL measured at 50 °C, than the later part of IRSL curve. Based on these observations, the thermal stability of the post-IR IRSL signal stimulated at elevated temperatures (100–200 °C) was also investigated. It was found that at least two groups of traps (shallow and deep) are associated with the IRSL and post-IR IRSL signals. The IRSL signal obtained at 50 °C is mainly from the shallow traps while the post-IR IRSL obtained at elevated temperatures is mainly from the deep traps. The kinetics parameters obtained using pulse annealing test indicate that the shallow IRSL traps are probably associated with the ∼300–350 °C TL peak and the deep traps are probably associated with the ∼400 °C TL peak. The shallow traps (∼350 °C TL peak) are associated with those easy-to-fade traps and the deep traps (∼400 °C TL peak) are associated with hard-to-fade traps.

Keywords

k, feldspar, infrared, stimulated, stability, luminescence, thermal, sedimentary, CAS

Disciplines

Medicine and Health Sciences | Social and Behavioral Sciences

Publication Details

Li, B. & Li, S. (2011). Thermal stability of infrared stimulated luminescence of sedimentary K-feldspar. Radiation Measurements, 46 (1), 29-36.

Thermal stability of infrared stimulated luminescence of sedimentary K-feldspar

Bo Li and Sheng-Hua Li

Department of Earth Sciences, The University of Hong Kong, Pokfulam Road, Hong Kong, China

Abstract

The thermal stability of the infrared stimulated luminescence (IRSL) signal measured at 50 °C as a function of IR stimulation time was investigated using KF grains extracted from sediments from central China. A dependence of thermal stability of IRSL signal on IR stimulation time and stimulation temperature was observed in pulse annealing studies. Relatively lower thermal stability is given by the initial part of the IRSL measured at 50 °C, than the later part of IRSL curve. Based on these observations, the thermal stability of the post-IR IRSL signal stimulated at elevated temperatures (100-200°C) was also investigated. It was found that at least two groups of traps (shallow and deep) are associated with the IRSL and post-IR IRSL signals. The IRSL signal obtained at 50°C is mainly from the shallow traps while the post-IR IRSL obtained at elevated temperatures is mainly from the deep traps. The kinetics parameters obtained using pulse annealing test indicate that the shallow IRSL traps are probably associated with the ~300-350°C TL peak and the deep traps are probably associated with the ~400°C TL peak. The shallow traps (~350°C TL peak) are associated with those easy-to-fade traps and the deep traps (~400°C TL peak) are associated with hard-to-fade traps.

Keywords: K-feldspar, luminescence, thermal stability, pulse annealing, anomalous fading.

1 Introduction

The infrared (IR) stimulated luminescence (IRSL) from sedimentary feldspar has been used for optical dating of sediment for the last two decades since the first report of optical stimulation spectra of feldspar by Hütt *et al* (1988). One of the critical assumptions in optical dating is that the trapped electrons used for dating are stable over the geological burial period. It is thus important to ensure that the IRSL signals are coming from deep traps with a long kinetic lifetime at ambient temperature (e.g. ~15°C). There have been several studies of the thermal stability of the IRSL signal from potassium-rich feldspar (KF) grains extracted from sediments (Li et al., 1997; Murray et al., 2009). It has been shown that the IRSL traps are associated with deep traps with a thermal depth of ~1.7 eV (Li et al., 1997), which have a lifetime of ~10^9 years. According to their isothermal studies, Murray et al. (2009) suggested that the IRSL traps of their KF sample is mainly originated from deep traps associated with the ~410°C peak. These studies focused on the initial part of the IRSL signal obtained by stimulating at ~50°C.

Although previous studies suggested that the IRSL signal from KF is thermally stable enough to allow for dating sediments over millions years (e.g. Li et al., 1997; Murray et al., 2009), the application of IRSL dating of KF has been hampered by the anomalous fading effect (Wintle, 1973), a phenomenon that the TL and IRSL signals decrease with storage at room temperature as a result of tunneling recombination (Spooner, 1992, 1994; Huntley and Lamothe, 2001; Huntley, 2006; Huntley and Lian, 2006; Li and Li, 2008).

Recent studies suggested different luminescence behaviours for the IRSL signal as a function of IR stimulation time (Thomsen et al., 2008; Li, in press). Particularly, it was observed that the initial part of the IRSL signal has a higher anomalous fading rate when compared to the later part (Thomsen et al., 2008), which was explained as that the emission of IRSL is a result of electron-hole recombination via tunnelling process under IR stimulation. This observation has led to the development of post-IR IRSL dating method, in which an IRSL bleaching at low temperature (~50°C) is applied before a high temperature (>200°C) IRSL measurement to reduce the fading rate of feldspar (Thomsen et al., 2008; Buylaert et al., 2009). In a recent study, Li (accepted) observed a strong dependence of thermal assistant energy on IR stimulation time; this was explained as that the initial part of IRSL signal is dominated by tunnelling recombination while the later part is dominated by thermal assisted recombination. All these studies indicate that different recombination processes are involved. It is thus necessary to further investigate the source of IRSL, as a function of IR stimulation conditions (i.e. stimulation time and temperature), before a reliable IRSL signal could be used for dating.

In this study, the thermal stability of the IRSL signal as a function of IR stimulation time is investigated using KF grains extracted from sediments from China. The trap parameters of the IRSL and post-IR IRSL signal stimulated at elevated temperatures (100-200°C) were also measured using pulse annealing with various heating rates. The relationship between anomalous fading, thermoluminescence (TL) and IRSL signal from KF are studied.

2 Samples and experimental details

Two Aeolian sedimentary samples (Sm1 and Sm7) from the transition zone between the Mu Us Desert and the Loess plateau in central China were used in this study (Sun et al., 1999). The age of Sm1 (~10 ka) has been determined using OSL dating of quartz and isochron IRSL (iIRSL) dating of K-feldspar (Li et al., 2008). The age of Sm7 (~440 ka) was estimated by correlation between stratigraphy and OIS stages (Li and Li, 2008). Previous study on the equivalent dose of the samples from the section suggested that the IRSL signal for sample Sm7 has reached an equilibrium state, i.e. the IRSL traps were in equilibrium between electron filling and escaping (or fading) (Li and Li, 2008). This is so-called “field saturation” (Lamothe et al., 2003; Huntley and Lian, 2006).

The samples were routinely treated with HCl and H_2O_2 to remove carbonate and organic matter in subdued red safe-light conditions. After drying, 150-180 μm grains were obtained by sieving. The KF grains were separated using heavy liquids with a density of 2.58 g/cm^3. The extracted KF grains were cleaned using 10% HF for 5 minutes. Aliquots containing several hundred grains were prepared by mounting the grains in a monolayer on a 9.8 mm diameter aluminum disc with "Silkospay" silicone oil. The IRSL measurements were made on an automated Risø TL-DA-12 reader equipped with IR diodes (880 nm, 40 mW/cm^2) for stimulation. Irradiations were carried out within the reader using a ^{90}Sr/^{90}Y beta source. The IRSL and TL signals were detected using a photomultiplier tube with the IRSL passing through a filter pack containing Schott BG-39 and Corning 7-59 filters, which allows for a blue violet transmission (320-480 nm).

3 Results

3.1 Pulse annealing test of IRSL at low temperature

A pulse annealing study was conducted to test whether there is a dependence of the thermal stability of IRSL signal on IR stimulation time. One IR-bleached aliquot of KF from sample Sm1 was given a regenerative dose of 38 Gy. It was first preheated at 250°C for 60 s, and then heated to a temperature T °C before the remaining IRSL signal (L_x) was measured at 50 °C for 100 s. Any sensitivity change was monitored by measuring the IRSL signal (T_x) from a test dose (12 Gy) after measurement of L_x. The same preheat condition (250°C for 60 s) was applied for the test dose IRSL measurement. This cycle was repeated by increasing the annealing temperature (T) from 160 to 500 °C in steps of 20°C. Fig. 1 shows the normalized sensitivity-corrected IRSL signal (L_x/T_x) remained after each temperature. The IRSL signals at different IR stimulation time were calculated and were shown as different curves (Fig. 1). It is found that different parts of the IRSL signal have different pulse annealing patterns. Particularly, the initial parts start to decrease at a slightly lower temperature than the later parts, indicating a different thermal stability for them. It should be noted that, the decrease of the IRSL signal after annealing is unlikely to be that the preceding TL recombination has changed the IRSL recombination probability. In this pulse-annealing study for IRSL, a test dose was applied to monitor the sensitivity change (i.e. a result of changing recombination probability), and any loss of IRSL due to changing recombination probability can be corrected by the test dose IRSL. This can be further supported by the observation that there is little dependent of De value on preheat temperature up to 300 °C for our samples (Li et al., 2007), which also rule out the contribution of IRSL signal from traps below 300°C.

3.2 Pulse annealing test of post-IR IRSL at high temperatures

It has been suggested that the post-IR IRSL measured at high temperatures (> 200°C) has a lower anomalous fading rate then the IRSL measured at low temperatures (~50°C) (Thomsen et al., 2008; Buylaert et al., 2009). However, it is still not clear whether they come from the same group of traps or not. To understand the post-IR IRSL measured at high temperatures better, a pulse annealing procedure outlined in Table 1 was conducted. Different from Thomsen et al. (2008), instead of directly increasing the IR stimulation temperature to a higher temperature after an IRSL measurement at 50°C, we progressively increased the IR stimulation temperatures in steps of 50°C, so that the IRSL and post-IR IRSL at different stimulation temperatures could be obtained after the same pre-treatments and using the same aliquot (Table 1). The normalized IRSL and post-IR IRSL curves obtained for each stimulation temperature were shown in Fig. 2(a). A significant increase in IRSL signal was observed when the stimulation temperature was increased, i.e. at 100 s (from 50 to 100 °C), 200s (from 100 to 150 °C) and 300s (from 150 to 200 °C).

In the pulse annealing study, an aliquot from sample Sm1 was first heated to 500 °C to empty all IRSL traps. It was then given a regenerative dose of ~38 Gy before a cut-heat to 300°C. It is noted that the reason for using this cut-heat to 300°C prior to the pulse-annealing procedure is to ensure that the effect of the TL signal on the high-temperature post-IR IRSL signal is negligible. The aliquot was then heated to a temperature (T°C) before four IRSL measurements at 50, 100, 150 and 200°C, respectively. After that, a test dose of ~12 Gy was given and the IRSL was measured at 50 and 200 °C, respectively, for monitoring any sensitivity change. This cycle was repeated by increasing the annealing temperature T from 160 to 500°C in steps of 20°C. It is found that there is little dependence of sensitivity on IR stimulation temperature, i.e. there is little difference between the changes in test dose IRSL at 50°C (step10 in Table 1) and that at 200°C (step11 in Table 1). Therefore, the test dose IRSL at 50°C (step10 in Table 1) was used to correct sensitivity changes for all the IRSL signals at different temperatures. To test the ability of the sensitivity correction by the test dose IRSL, a recycling measurement for the response of the 240°C annealing was applied at the end of the measurement of the pulse annealing cycle (i.e. the 500 °C annealing). A recycling ratio of 0.95±0.02 was obtained, suggesting that the sensitivity changes can be corrected appropriately using this procedure.

The sensitivity-corrected IRSL signal was plotted against annealing temperature in Fig. 2(b). The pulse annealing curve of the 50°C IRSL (blue curve) is identical to that shown in Fig. 1, although different preheating temperatures, i.e. 250 °C (Fig. 1) and 300 °C (Fig. 2), were used prior to annealing. This suggests that the preheating conditions up to 300°C have negligible effect to the pulse-annealing results. It is shown that the post-IR IRSL signals obtained at higher temperatures are more thermally stable than the IRSL signal measured at 50 °C (Fig. 2). The IRSL at 50°C start to decrease at ~300 °C, while the post-IR IRSL signal at 200°C is stable up to 350 °C. This result suggests that the IRSL and post-IR IRSL signals at elevated temperatures originated from different groups of traps with different thermal stabilities.

3.3 Trap parameters of IRSL and post-IR IRSL traps

Since the IRSL and post-IR IRSL signals at elevated temperatures appear to be originate from different groups of traps, it is thus necessary to measure the trap parameters related to the IRSL and post-IR IRSL traps. In this study, pulse annealing with different linear heating rates similar to that described by Li et al. (2007) was used to investigate the thermal stability and kinetic parameters of traps related to the IRSL and post-IR IRSL. A single aliquot of KF from sample Sm1 was heated to

500°C to remove all IRSL trapped charges and then measured using the same pulse annealing procedure outlined in Table 1 but with different heating rates (β=3, 2, 1 and 0.5 °C/s) in step 3.

Fig. 3a shows the pulse annealing curves for the IRSL at 50°C. As expected, the lower heating rate resulted in an earlier reduction in IRSL at lower temperature due to a longer effective heating period for lower heating rate. Similar trends were observed for the post-IR IRSL at elevated temperatures (100, 150 and 200°C). Fig. 3b shows the luminescence reduction rate (%/°C) as a function of temperature for the IRSL at 50°C obtained using the data sets in Fig. 3a. The luminescence reduction rate was calculated as the difference between the signals measured at T and that at (T-20°C). Because the reduction of luminescence between T and (T-20°C) is an average effect of heating from (T-20°C) to T, the average temperature for each heating from to (T-20°C) to T would be (T-10)°C. It is shown that the reduction of the IRSL and post-IR IRSL signals increase with annealing temperature and then reach a peak before the reduction rate decrease again (Fig. 3b). There is an apparent shift of peak positions toward to higher temperatures for post-IR IRSL at elevated temperatures, indicating a higher thermal stability for post-IRSL at elevated temperatures. Similar trends were observed for the post-IR IRSL at elevated temperatures (100, 150 and 200°C).

The reduction rate peak positions (T_m) were obtained by fitting the data sets in Fig. 3b using a Gaussian function and they were then used to calculate the trap parameters (activation energy *E* and frequency factor *s*) using the same procedure described by Li et al. (1997). The Arrhenius plots, $\ln(T_m^2/\beta)$ plotted against $1/kT$ (β is the heating rate and k is the Boltzmann constant), for all IRSL and post-IR IRSL at elevated temperatures were shown in Fig. 4. The calculated *E* and *s* values are summarized in Table 2. For the initial (0-1 s) IRSL measured at 50 °C, an energy depth of E=1.8±0.1 eV and corresponding frequency factor of $s=2.7\text{x}10^{13}$ s^{-1} were obtained, which predicts a TL peak temperature of ~370°C. These values are consistent with previous results using different KF samples, e.g. a value of 1.72 eV was reported by Li et al (1997). Murray et al. (2009) also measured E and s values for the IRSL signal using isothermal study and they determined a TL peak temperature of

430±30°C assuming first-order kinetics, which predicts a more stable trap source than our study. This discrepancy is probably due to the imperfect assumption of first-order kinetics and using different methods for estimating kinetic parameters. However, the predicted TL peak position based on the values in this study is consistent with experimental pulse annealing results (the peak of the percentage reduction curve), i.e. both peaks are at temperature around 370°C (Fig. 3b).

It is interesting to note that substantially larger values of E were obtained for all post-IR IRSL signals, i.e. the energy depth E was found to be 2.2±0.2, 2.5±0.2 and 2.4±0.2 eV for the post-IR IRSL signal measured at 100, 150 and 200 °C, respectively. Meanwhile, much larger *s* values in the magnitude of ~10^{16}-10^{17} s^{-1} were also obtained for these post-IR IRSL signals at elevated temperatures.

The kinetic parameters were used to predict the corresponding lifetimes and first-order TL peak positions (Aitken, 1985) for each signal and the results are summarized in Table 2. It is noted that the uncertainties of the kinetic parameters (E and s) result in a large uncertainty on the calculated peak temperatures so that a large range of TL peak temperature could be resulted. For example, a change of 0.2 eV in the value of E for the 150 °C post-IR IRSL trap could result in a ~50 °C change in the corresponding TL peak temperature. As a result, the calculated TL peak temperatures for different IRSL signals could overlap with each other. However, the reduction rate plot (Fig. 3b), which could be treated as an equivalent (or analogue) of TL peaks for each IRSL signal, were obtained experimentally and shows a significant difference among the peak positions of different IR stimulation temperatures and different heating rates (Fig. 3b). This discrepancy cannot be explained by experimental uncertainties. It is thus concluded that at least two groups of traps (shallow and deep) were identified to be associated with the IRSL and post-IR IRSL signals for our sample. One is the shallow trap corresponding to the initial IRSL signal measured at 50°C, which is predicted to be associated with a TL peak at ~370°C for a heating rate of 5°C/s. No distinctive difference was observed between the trap parameters for the post-IR IRSL signals at 100, 150 and 200°C; these could be associated with a similar TL peak centred at ~400°C at 5 °C/s. The slight shift of the peak position from ~392°C for the 100°C post-IR IRSL to ~415°C for the 200°C post-IR IRSL signal is reasonable because there might be more residual signal originating from the shallow traps for the 100°C post-IR IRSL than the 200°C post-IR IRSL All the traps are geologically stable according to the lifetimes (~10^{10} and ~10^{17} years, respectively) predicted from their kinetic parameters for the first order kinetics (Table 2).

3.4 Effects of IR bleaching on TL signal for field-saturated sample

3.4.1 Effects of IR bleaching on TL signal from natural and bleached sample

The field-saturated sample Sm7 was used to investigate the relationship between anomalous fading, TL and IR bleaching. Here the reduction of TL as a result of IR bleaching was used as an aid to study the potential sources of IRSL. Fig. 5a shows the natural TL signals (N) after a 60 s preheat at 250°C (blue curve), the remaining TL signal after preheating and IR bleaching at 50°C for 1000 s (N+IR) (red curve) and their difference (N-(N+IR)) (green curve). A single broad TL peak at ~365 °C was observed for the natural TL (N). The 1000 s IR bleaching resulted in a slight reduction in the peak intensity at higher temperature range (350-500°C) and increase in the lower temperature side (150-350°C) (Fig. 5a). This was expected as a result of photo-transfer of charges from deep IR-sensitive traps into shallow IR-insensitive traps. The main TL peak position shifted slightly from ~365°C for natural TL to ~355°C after IR bleaching. The difference between the two TL curves (N-(N+IR)), which represents the IR-bleachable TL signal, was also shown (green curve). A peak centred at ~400°C was obtained, indicating the main source of IR-bleachable TL signal in this field-saturated natural sample. Besides the main 400°C TL peak, a small shoulder at ~350°C, probably associated with another TL peak, could also be identified as IR-bleachable. A negative TL peak at ~270°C indicates the reservoir traps accepting the photo-transferred charges.

After measuring the natural TL, three aliquots were given a laboratory beta dose (β) of 470 Gy and then preheated at 250°C for 60 s. The TL signals with and without 1000 s IR bleaching were then measured. Fig. 5b shows the laboratory regenerative TL signals obtained without IR bleaching (β) (blue curve), after IR bleaching (β+IR) (red curve) and their difference (β-(β+IR)) (green curve). A similar TL peak at ~365°C was obtained for both the regenerative TL signal with and without IR bleaching. The reduction of the TL signal as a result of IR bleaching was shown as their difference (β-(β+IR)) (green curve in Fig. 5b). Two positive peaks centred at ~400 and 350°C could be identified as IR bleachable. A negative peak at ~270°C was also identified as photo-transferred signal. The IR-bleachable TL signals for both the natural and regenerative doses were compared in Fig. 5c. It is interesting to note that the relative magnitudes of the 400 and 350°C peaks in laboratory regenerative samples are significantly different from that obtained from the natural sample (Fig. 5c). For beta-regenerated TL signal (β-(β+IR)), there is a much higher proportion of IR-bleachable signals originated from the 350°C peak than that from the natural sample (Fig. 5c). Only a small proportion of IR-bleachable signals was identified from the 350°C peak for natural TL signal (N-(N+IR)). This result indicates that there are different proportions of IR-bleachable TL signals from the 350 and 400°C TL peaks for natural samples and laboratory-irradiated samples.

3.4.2 Effects of IR bleaching on TL signal from N+ β sample

It has been shown that the natural signal has a different anomalous fading rate from the laboratory irradiated samples (Li and Li, 2008; Kars et al., 2008). In an extreme case, for a field-saturated sample, the signals generated by laboratory beta irradiation above the natural dose are dominated by the fading (geologically unstable) signals, while the natural signal are dominated by the non-fading (stable) signal (Li and Li, 2008). To better understand the anomalous fading in feldspar, the effect of IR bleaching on TL signal was investigated using the naturally saturated (or field-saturated) sample Sm7. Three natural aliquots were first given a beta dose of 470 Gy above their natural dose (620 ± 21 Gy, Li and Li, 2008) as (N+β). The aliquots were then preheated at 250°C for 60 s before their TL curves were measured. The TL curve of N+β (red curve) was compared with natural TL curve (N) (blue curve) in Fig. 6a. The difference between them (green curve) thus represents the β-generated signal above the natural TL. It is shown that, different from the TL curves of N and N+β, two peaks were identified in the β-generated signal. There is a distinctive peak (shoulder) at ~310°C. One possible explanation for this is that the fading signal is associated with the low temperature peak. Another test for this is to compare the TL curve obtained immediately after irradiation and that measured after storage (Figure 7). It is shown that the lost TL signal after storage for ~2 days is dominated by a single peak at ~340°C. Because the complexity of mineralogy and luminescence emissions involved, there is a lack of firm evidences for the direct link between IRSL and TL signals, our results indicate that the shallow traps of ~350 °C TL peak is relatively easier to fade anomalously than the deep traps of the ~400 °C TL peak.

More relative information on the anomalous fading characteristics of TL and IRSL signals could be revealed by studying the effect of IR bleaching on the TL signal of N+β samples. Three aliquots from Sm7 were treated similarly as above, i.e. they were given a dose β above the natural N. After preheat, they were bleached for 1000 s by IR at 50 °C before TL measurements (N+β+IR). The TL curve from N+β+IR (red curve) was compared with that from N+β (blue curve) in Fig. 6b. Two distinctive peaks, at ~330 and ~380 °C, were identified in the difference between these two curves (green curve in Fig. 6b), which represents the IR-bleachable signals in the TL from the N+β. In Fig. 6c, the IR-bleachable TL signal from N+β was compared with that from N (green curve in Fig. 5a). As shown, a significant difference is observed between the two curves (Fig. 6c). There is a significantly larger reduction in the TL signal from the low temperature range (300-350 °C) for the N+β sample as a result of IR bleaching when compared to that from the natural sample (N). The difference between these two curves shows a distinctive peak at 300-350 °C (green curve in Fig. 6c), which represents the IR-bleachable β-generated TL signal above the natural dose. A possible explanation to this result is that the IR-bleachable signals from the natural sample (N) and the natural+beta (N+β) sample have different contributions from the shallow traps (300-350 °C TL peak) and deep traps (~400°C TL peak). relationship between IRSL and TL deserves for further study.

4 Discussions

At least two groups of IRSL traps have been identified in the pulse annealing study of the IRSL and post-IR IRSL at elevated temperatures (section 3.2). The initial part of the IRSL measured at 50°C was shown to be dominated by a group of shallow traps with an apparent trap depth of ~1.8 eV, while the post-IR IRSL at elevated temperatures (>100°C) was dominated by deep traps with an apparent depth of ~2.3 eV. It is noted that these values were obtained by assuming first-order kinetics and a single trap for the IRSL at each stimulation temperature. These values might not be correct when there are two or more traps envolved in the production of IRSL signal at different temperatures, which is the case indicated from our results in section 3.4. However, such values can still provide a prediction of the thermal behaviour of the IRSL signals. For example, the kinetic parameters obtained for the two groups of IRSL traps predict two TL peaks centred at ~360 °C and ~400°C. This is consistent with the results obtained from the studies in IR bleaching of TL glow curves (section 3.4), in which the IR bleaching resulted in reduction in two distinctive peaks at ~350 °C and ~400 °C in the TL signal (Fig. 5c).

The TL and IRSL signals from feldspar have been shown to decrease with storage at room temperature due to the anomalous fading effect (Wintle, 1973), even though the relevant trapped electrons are thermally stable over geologically-long periods of time. The anomalous fading process has been shown to be a result of direct recombination of electron-hole pairs via tunnelling (Aitken, 1985; Visocekas, 1985; Visocekas et al., 1994). Assuming a random distribution of traps, those close-by electron-hole pairs will be preferentially recombined (Huntley, 2006). For the field-saturated sample Sm7, all the stable (non-fading) traps distant from recombination centres have already been filled, while those traps in close proximity to recombination centres are approximately empty because the probability of tunnelling is higher than that of trap filling (Li and Li, 2008). Therefore, the natural IRSL signal (N) from Sm7 represents the recombination from spatially distant electron-hole pairs (non-fading), while the IRSL signal from the laboratory irradiated natural sample (N+β) was a result of the combination of both close pairs (fading) and distant pairs. It has been shown that the IRSL signal from N+β sample ($L_β$) has a very high fading rate of ~11 %/decade (Li and Li, 2008). Our results show that the IR-bleachable TL signal from N+β sample has a significantly higher contribution from the ~350 °C TL peak, when compared to the IR-bleachable TL signal from the natural sample (N) that is dominated by the ~400 °C TL peak (Fig. 6c). It is therefore expected that the shallow traps of the TL peak at ~350 °C has a higher fading rate than the deep traps of the TL peak at ~400°C. To test this, the reduction of TL signal as a result of storage at room temperature was conducted. It is shown that there was a significant reduction in the TL signal in the low temperature range (peaked at 300-350°C) after storage for ~2 days, while little reduction was observed in the TL signal at ~400°C (Fig. 7a). To quantify the fading rate of the TL signal in different temperature ranges, a fading test procedure similar to that described by Auclair et al (2003) was applied to measure the fading rate (g value) using sample Sm1 (Fig. 7b). The g value for the TL signal integral in the range of 301-350°C was estimated to be 3.3±0.3 %/decade. However, a much lower fading rate of 1.7±0.4 %/decade was obtained for the signal integral in the range of 381-420°C, although a higher relative uncertainty was obtained for this temperature range (Fig. 7b).

Despite of the lack of a firm and direct link between IRSL and TL signals from K-feldspar, the results from this study give indications that the IRSL signals from KF may be associated with two TL peaks at ~350°C and ~400 °C. Given by the different anomalous fading characteristics of the two TL peaks (Fig. 7), our results may partly explain the phenomenon that the post-IR IRSL at elevated temperatures has a lower fading rate than the initial part of the IRSL signal at 50°C (Thomsen et al., 2008), because the former was dominated by the deep traps associated with the ~400°C TL peak while the latter was dominated by the shallow traps associated with the ~350°C TL peak (Table 2). Therefore, the dependence of anomalous fading rate on IR stimulation time and temperature, as observed by previous studies (Thomsen et al., 2008), can be attributed to the fact that different groups of traps with different anomalous fading rates have contributed to the IRSL and their relative contribution changes as a function of IR stimulation time and temperature.

5 Conclusions and implications for luminescence dating

The results presented in our study show that at least two groups of traps (shallow and deep) are associated with the IRSL signals. The shallow IRSL traps are probably associated with the ~350°C TL peak and the deep traps are probably associated with the ~400°C TL peak. The initial part of IRSL signal obtained at 50°C is mainly from the shallow traps while the post-IR IRSL obtained at elevated temperatures is mainly from the deep traps, suggesting a preferentially bleaching of the shallow traps compared to the deep traps under IR stimulation. Since the 350°C TL peak is associated with those easy-to-fade traps and the ~400°C TL peakis associated with hard-to-fade traps (Fig. 7a and b), it is expected that the post-IR IRSL could be used to select the hard-to-fade signals associated with the deep traps for dating, which has been suggested by Thomsen et al. (2008). It can be expected that choosing the most appropriate preheat and stimulation conditions may be able to select a non-fading signal for dating purpose.

Acknowledgements

Prof. Jimin Sun is thanked for helping with sample collection. Dr. Jakob Wallinga and an anonymous referee are appreciated for providing valuable comments on the manuscripts. This study was financially supported by the grants to Sheng-hua Li from the Research Grant Council of the Hong Kong Special Administrative Region, China (Project no. 7035/06P, 7035/07P and 7028/08P) and the "small project funding" grant to Bo Li from the University of Hong Kong (Project code. 200807176166).

References

Aitken, M.J., 1985. *Thermoluminescence dating*. Academic press London.

Buylaert, J.P., Murray, A.S., Thomsen, K.J., Jain, M., 2009. Testing the potential of an elevated temperature IRSL signal from K-feldspar. *Radiation Measurements* **44**, 560-565.

Hütt, G., Jaek, I., Tchonka, J., 1988. Optical dating: K-feldspars optical response stimulation spectra. *Quaternary Science Reviews* **7**, 381-385.

Huntley, D.J., 2006. An explanation of the power-law decay of luminescence. *Journal of Physics-Condensed Matter* **18**, 1359-1365.

Huntley, D.J., Lamothe, M., 2001. Ubiquity of anomalous fading in K-feldspars and the measurement and correction for it in optical dating. *Canadian Journal of Earth Sciences* **38**, 1093-1106.

Huntley, D.J., Lian, O.B., 2006. Some observations on tunnelling of trapped electrons in feldspars and their implications for optical dating. *Quaternary Science Reviews* **25**, 2503-2512.

Kars, R.H., Wallinga, J., Cohen, K.M., 2008 A new approach towards anomalous fading correction for feldspar IRSL dating – tests on samples in field saturation. *Radiation Measurements* **43,** 786-790.

Lamothe, M., Auclair, M., Hamzaoui, C., Huot, S., 2003. Towards a prediction of long-term anomalous fading of feldspar IRSL. *Radiation Measurements* **37**, 493-498.

Li, B. The relationship between thermal activation energy, infrared stimulated luminescence and anomalous fading of K-feldspars. *Radiation Measurements* (in press).

Li, B., Li, S.H., 2008. Investigations of the dose-dependent anomalous fading rate of feldspar from sediments. *Journal of Physics D-Applied Physics* **41**, 225502.

Li, B., Li, S.H., Wintle, A.G., Zhao, H., 2007. Isochron measurements of naturally irradiated K-feldspar grains. *Radiation Measurements* **42**, 1315-1327.

Li, B., Li, S.H., Wintle, A.G., Zhao, H., 2008. Isochron dating of sediments using luminescence of K-feldspar grains. *Journal of Geophysical Research-Earth Surface* **113**, F02026, doi:02010.01029/02007JF000900. .

Li, S.H., Tso, M.Y.W., Wong, N.W.L., 1997. Parameters of OSL traps determined with various linear heating rates. *Radiation Measurements* **27**, 43-47.

Murray, A.S., Buylaert, J.P., Thomsen, K.J., Jain, M., 2009. The effect of preheating on the IRSL signal from feldspar. *Radiation Measurements* **44**, 554-559.

Spooner, N.A., 1992. Optical Dating: preliminary results on the anomalous fading of luminescence from feldspars. *Quaternary Science Reviews* **11**, 139-145.

Spooner, N.A., 1994. The anomalous fading of infrared-stimulated luminescence from feldspars. *Radiation Measurements* **23**, 625-632.

Sun, J.M., Ding, Z.L., Liu, T.S., Rokosh, D., Rutter, N., 1999. 580,000-year environmental reconstruction from aeolian deposits at the Mu Us Desert margin, China. *Quaternary Science Reviews* **18**, 1351-1364.
Thomsen, K.J., Murray, A.S., Jain, M., Bøtter-Jensen, L., 2008. Laboratory fading rates of various luminescence signals from feldspar-rich sediment extracts. *Radiation Measurements* **43**, 1474-1486.
Visocekas, R., 1985. Tunneling radiative recombination in labradorite : its association with anomalous fading of thermoluminescence. *Nuclear Tracks and Radiation Measurements* **10**, 521-529.
Visocekas, R., Spooner, N.A., Zink, A., Blanc, P., 1994. Tunnel afterglow, fading and infrared-emission in thermoluminescence of feldspars. *Radiation Measurements* **23**, 377-385.
Wintle, A.G., 1973. Anomalous Fading of Thermoluminescence in Mineral Samples. *Nature* **245**, 143-144.

Table 1 Pulse annealing procedure for IRSL and post-IR IRSL at elevated temperatures.

Step	Treatment	Observed
1	Regenerative dose (38 Gy)	
2	Cut-heat to 300°C	
3	Cut-heat to T°C (T=160-500°C)	
4	IRSL measurement at 50°C for 100 s	L_{50}
5	IRSL measurement at 100°C for 100 s	L_{100}
6	IRSL measurement at 150°C for 100 s	L_{150}
7	IRSL measurement at 200°C for 100 s	L_{200}
8	Test dose (12 Gy)	
9	Cut-heat to 300°C	
10	IRSL measurement at 50°C for 100 s	T_{50}
11	IRSL measurement at 200°C for 100 s	T_{200}
12	Cut-heat to 500°C	
13	Return to step 1 and T=T+20°C	

Table 2 The kinetic parameters obtained from the data sets in Fig. 4, and the predicted lifetimes and first-order TL peak positions calculated using the values of E and s. The TL peak was calculated using a heating rate of 5 °C/s.

Signal type	**E (eV)**	**s (s^{-1})**	**Lifetime at 20°C (years)**	**TL peak (°C)**
IRSL at 50°C	1.8±0.1	$2.7x10^{13}$	$1.0x10^{10}$	373
Post-IR IRSL at 100°C	2.2±0.2	$2.2x10^{16}$	$9.5\ x10^{13}$	392
Post-IR IRSL at 150°C	2.5±0.2	$8.4x10^{17}$	$3.6x10^{17}$	410
Post-IR IRSL at 200°C	2.4±0.2	$1.1x10^{17}$	$5.3x10^{16}$	415

Figure captions

Figure 1: The normalized sensitivity-corrected IRSL signal (L_i/T_i) as a function of the annealing temperature (T) for different IR stimulation time (0-1, 5-6, 10-11, 15-16, 50-51 and 80-81 s). The heating rate used is 3 °C/s. All curves were normalized to the initial value. All the IRSL signals (L_i and T_i) are calculated from the integral of the counts in the time periods shown, with subtraction of an equivalent background obtained in the last 5 s of the IRSL curves.

Figure 2: (a) The normalized IRSL and post-IR IRSL curves obtained for different stimulation temperature (temperatures are shown above each curve). All IRSL curves were normalized to the initial stimulation at t=0. (b) Pulse annealing results from the IRSL and post-IR IRSL at different temperatures obtained using the procedure in Table 1. The corrected IRSL signal was calculated using the ratio of the IRSL signals (L_{50}, L_{100}, L_{150} and L_{200}) to the test dose IRSL signal (T_{50}). The heating rate for each heating is 2°C/s. All curves were normalized to the initial value. All the IRSL and post-IR IRSL signals (L_i and T_i) are calculated from the integral of the counts in the initial 1 s, with subtraction of an equivalent background obtained in the last 5 s of the IRSL curves.

Figure 3: (a) Pulse annealing curves using different heating rates for the IRSL measured at 50°C; All IRSL signals were normalized to the initial value. All the IRSL and post-IR IRSL signals (L_i and T_i) are calculated from the integral of the counts in the initial 1 s, with subtraction of an equivalent background obtained in the last 5 s of the IRSL curves. (b) The luminescence reduction rate (%/°C) obtained using the data sets in (a). The luminescence

reduction rate was plotted as a function of the average temperature for each heating, i.e. (T-10)°C. All curves had been smoothed using three-point running mean.

Figure 4: The Arrhenius plots, $\ln(T_m^2/\beta)$ plotted against $1/kT$, for IRSL at 50°C, post-IR IRSL at 100°C, 150°C and 200°C. β is the heating rate used in pulse annealing tests. k is the Boltzmann constant. T_m is the reduction rate peak positions.

Figure 5: (a) The natural TL signals (N) after a 60 s preheat at 250°C (blue curve), the remained TL signal after preheating and IR bleaching at 50°C for 1000 s (N+IR) (red curve) and their difference (N-(N+IR)) (green curve). (b) The TL signals from laboratory-irradiated sample (β) (blue curve), and IR-bleached laboratory-irradiated sample (β+IR) (red curve) and their difference (β -(β+IR)) (green curve). (c) Comparison of the IR-bleachable TL signals from natural sample (N-(N+IR)) (blue curve) and laboratory-irradiated sample (β -(β+IR)) (green curve). The signal of (β -(β+IR)) was multiplied by a factor of 3 for a better comparison. All TL curves were measured using a heating rate of 5°C/s. Each curve was obtained from the average of three paralleled aliquots. The inter-aliquot variation of TL curves from different aliquots was normalized using the natural IRSL signal obtained by a short exposure to IR at a reduced intensity (10%) before any measurement.

Figure 6: (a) The TL curve of N+β (red) sample compared with the natural TL curve (N) (blue curve), and their difference ((N+β)-N) (green). (b) The TL curve of IR-bleached N+β sample (N+β+IR) (red curve) compared with the TL curve of N+β sample (blue), and their difference

((N+β)-(N+β+IR)) (green). (c) Comparison of the IR-bleachable TL signals from N+β sample (N+β -(N+β +IR)) (blue), natural sample (N-(N+IR)) (red), and their difference (green). All TL curves were measured using a heating rate of 5°C/s. Each curve was obtained from the average of three paralleled aliquots. The inter-aliquot variation of TL curves from different aliquots was normalized using the natural IRSL signal obtained by a short exposure to IR at a reduced intensity (10%) before any measurement.

Figure 7: (a) The TL curves of laboratory irradiated sample. The red curve (prompt) was obtained immediately following irradiation. The blue curve (delayed) was obtained after a storage of ~2 days (blue). The green curve shows the difference between the prompt and delayed curves. For a better comparison, the difference between the prompt and delayed curves was multiplied by a factor of 10. All the curves were obtained using the same aliquot of Sm7. The aliquot was heated to 500°C before giving laboratory dose (46 Gy). The TL curves were measured using a heating rate of 5°C/s. (b) Anomalous fading test of the TL signals in the ranges of 301-350 °C and 381-420°C as a function of delayed period (t). The normalized TL signals were obtained using the delayed L_i/T_i method as described by Auclair et al. (2003) with each IRSL measurement in the procedure replaced by 500°C TL measurement. The regeneration dose and test dose are 32 Gy and 8 Gy, respectively. A preheat at 250°C for 60 s was applied before TL measurement to empty shallow TL traps. The corrected TL signals (L_i/T_i) were normalized to the first measurement (t_c=430 s). The calculated g values are shown in the figure. The data sets were derived using four KF aliquots from sample Sm1.

Figure 1

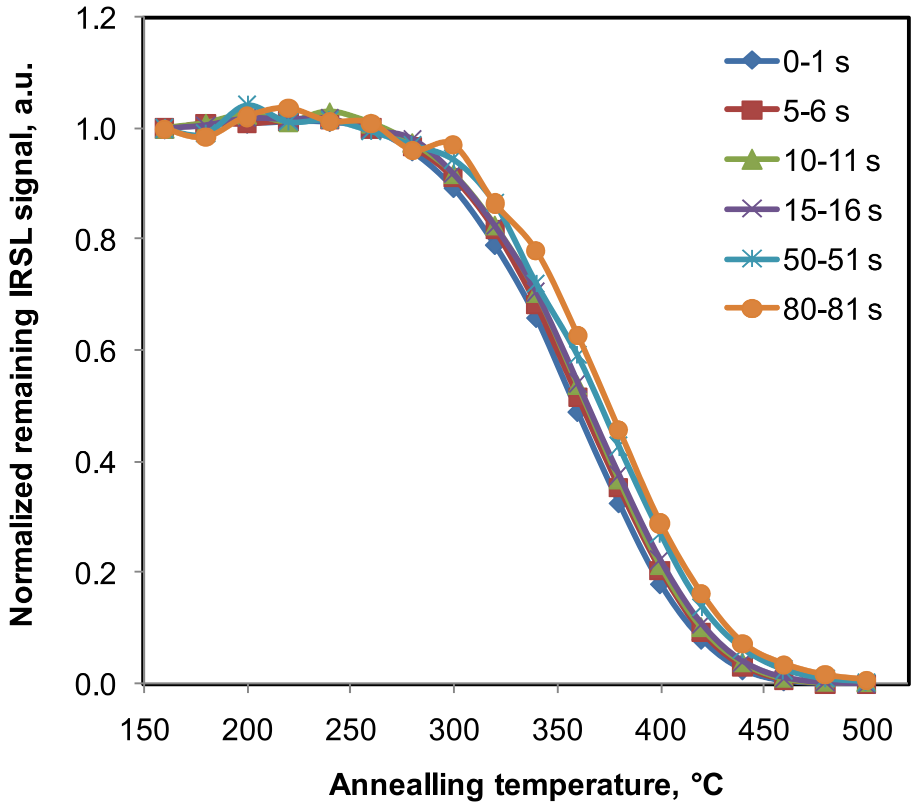

1.2
1.0
0.8
0.6
0.4
0.2
0.0
Normalized remaining IRSL signal, a.u.
150
200
250
300
350
400
450
500
Annealling temperature, °C
0-1 s
5-6 s
10-11 s
15-16 s
50-51 s
80-81 s

Figure 2

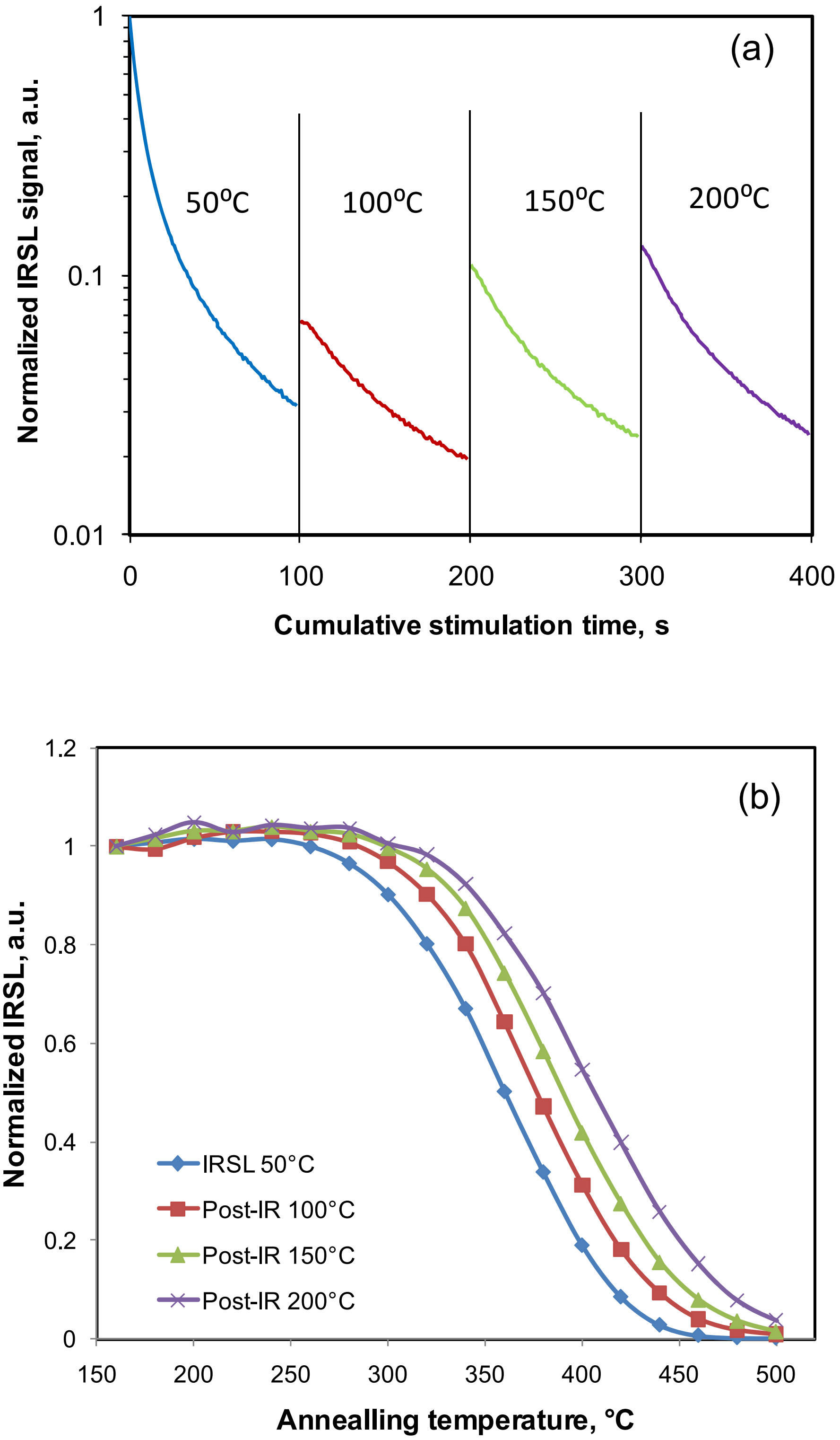
(a)
50°C
100°C
150°C
200°C
1
0.1
0.01
0
100
200
300
400
Normalized IRSL signal, a.u.
Cumulative stimulation time, s
(b)
1.2
1
0.8
0.6
0.4
0.2
0
150
200
250
300
350
400
450
500
IRSL 50°C
Post-IR 100°C
Post-IR 150°C
Post-IR 200°C
Normalized IRSL, a.u.
Annealling temperature, °C

Figure 3

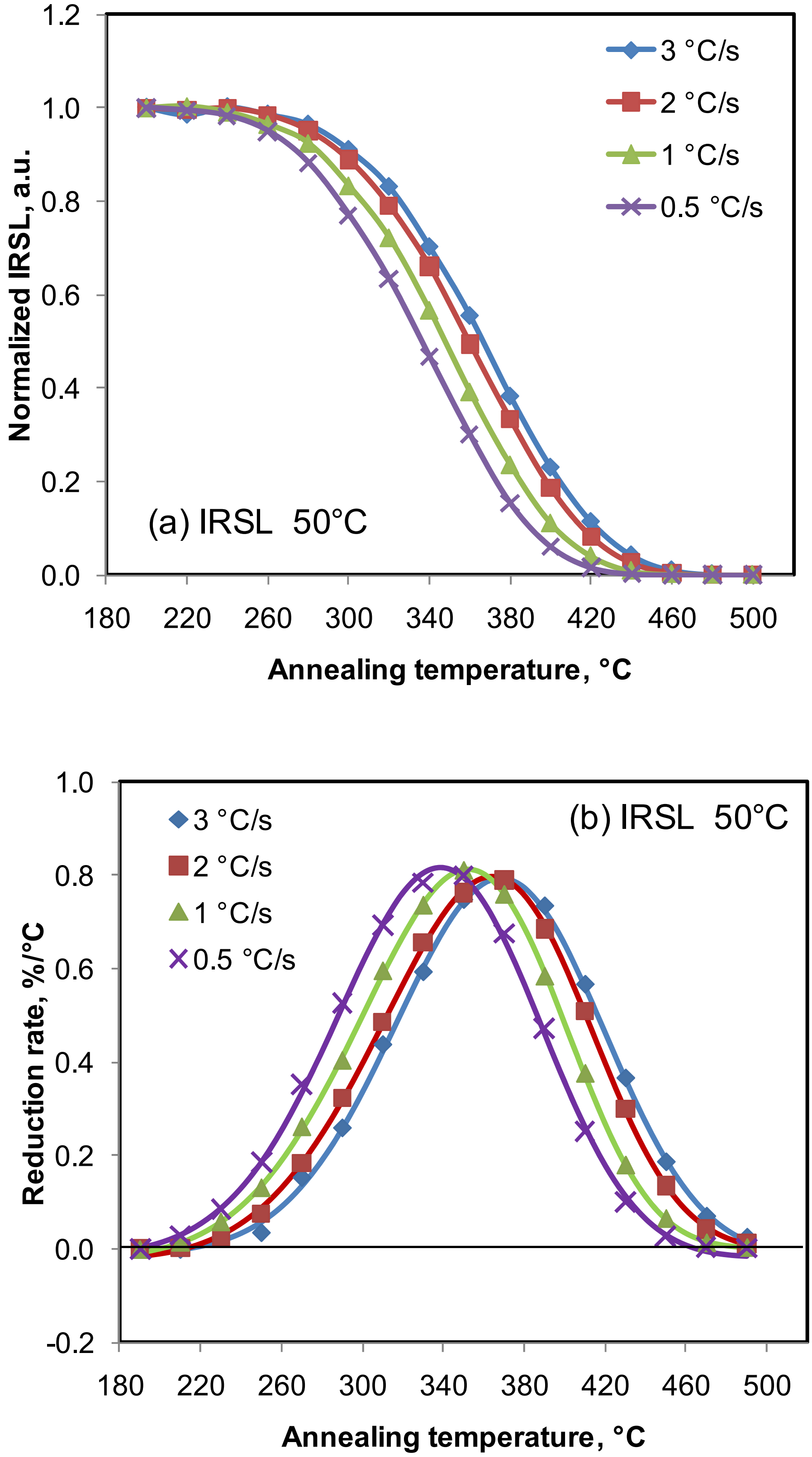

3 °C/s
2 °C/s
1 °C/s
0.5 °C/s
(a) IRSL 50°C
Normalized IRSL, a.u.
1.2
1.0
0.8
0.6
0.4
0.2
0.0
180 220 260 300 340 380 420 460 500
Annealing temperature, °C
3 °C/s
2 °C/s
1 °C/s
0.5 °C/s
(b) IRSL 50°C
Reduction rate, %/°C
1.0
0.8
0.6
0.4
0.2
0.0
-0.2
180 220 260 300 340 380 420 460 500
Annealing temperature, °C

Figure 4

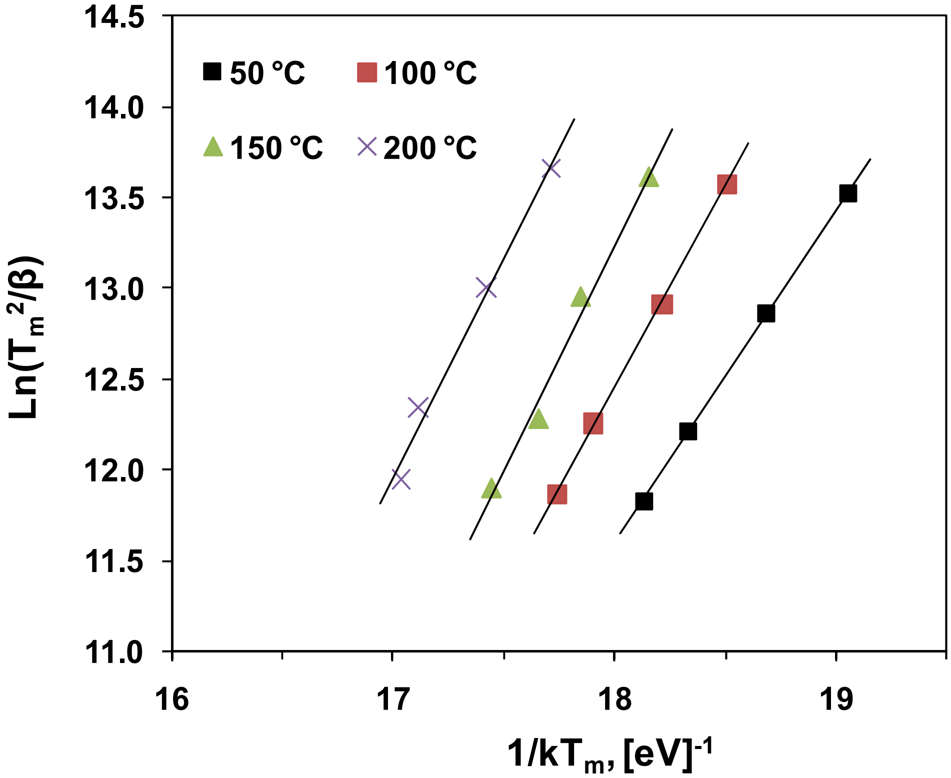

50 °C
100 °C
150 °C
200 °C
14.5
14.0
13.5
13.0
12.5
12.0
11.5
11.0
16
17
18
19
Ln(Tm2/β)
1/kTm, [eV]-1

Figure 5

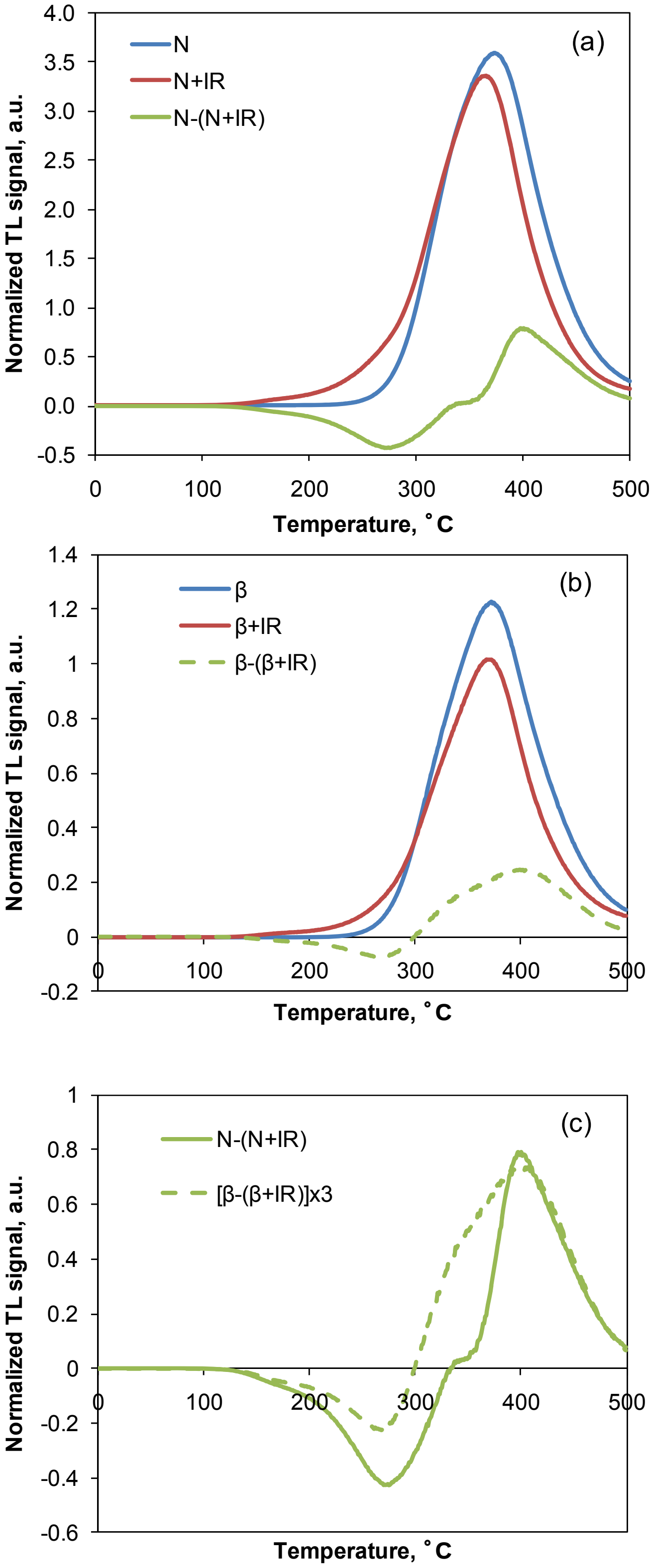

(a)
N
N+IR
N-(N+IR)
Normalized TL signal, a.u.
Temperature, ˚C
(b)
β
β+IR
β-(β+IR)
Normalized TL signal, a.u.
Temperature, ˚C
(c)
N-(N+IR)
[β-(β+IR)]x3
Normalized TL signal, a.u.
Temperature, ˚C

Figure 6

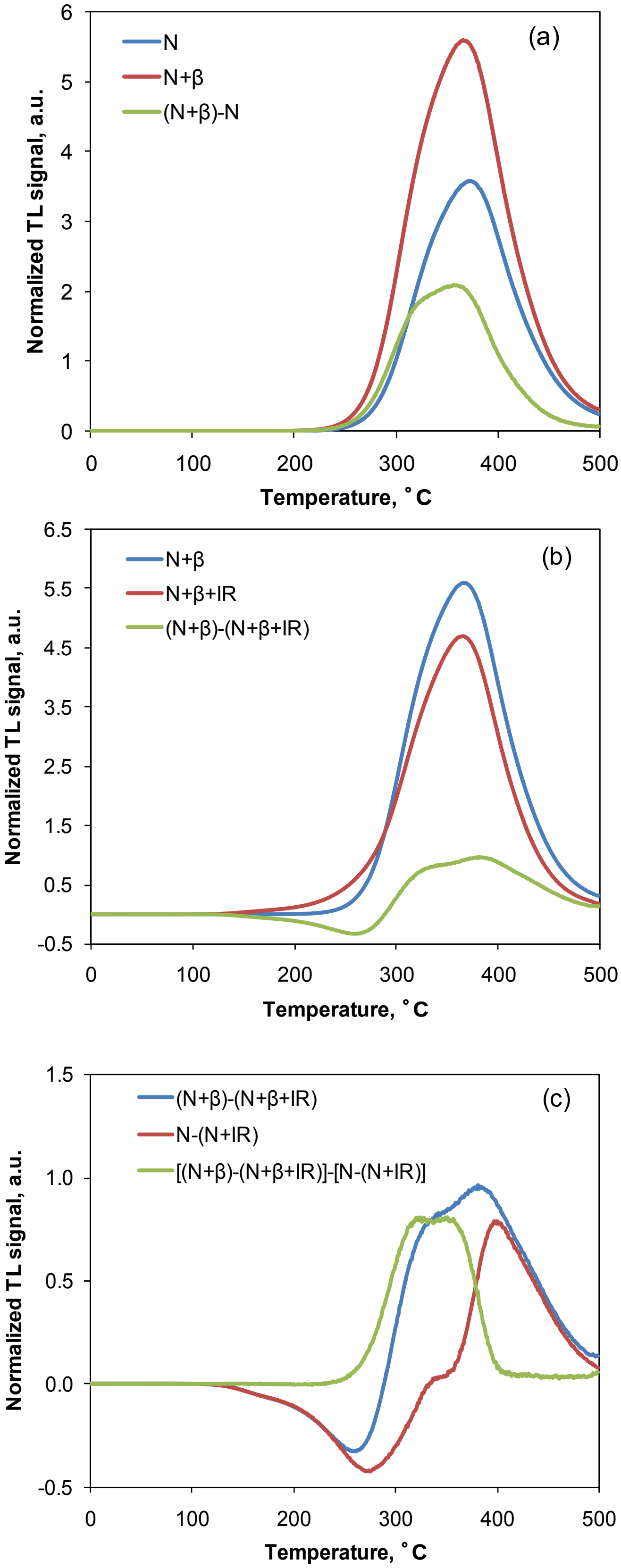

(a)
N
N+β
(N+β)-N
Normalized TL signal, a.u.
Temperature, ˚C
0
1
2
3
4
5
6
100
200
300
400
500
(b)
N+β
N+β+IR
(N+β)-(N+β+IR)
-0.5
0.5
1.5
2.5
3.5
4.5
5.5
6.5
(c)
(N+β)-(N+β+IR)
N-(N+IR)
[(N+β)-(N+β+IR)]-[N-(N+IR)]
0.0
0.5
1.0
1.5

Figure 7

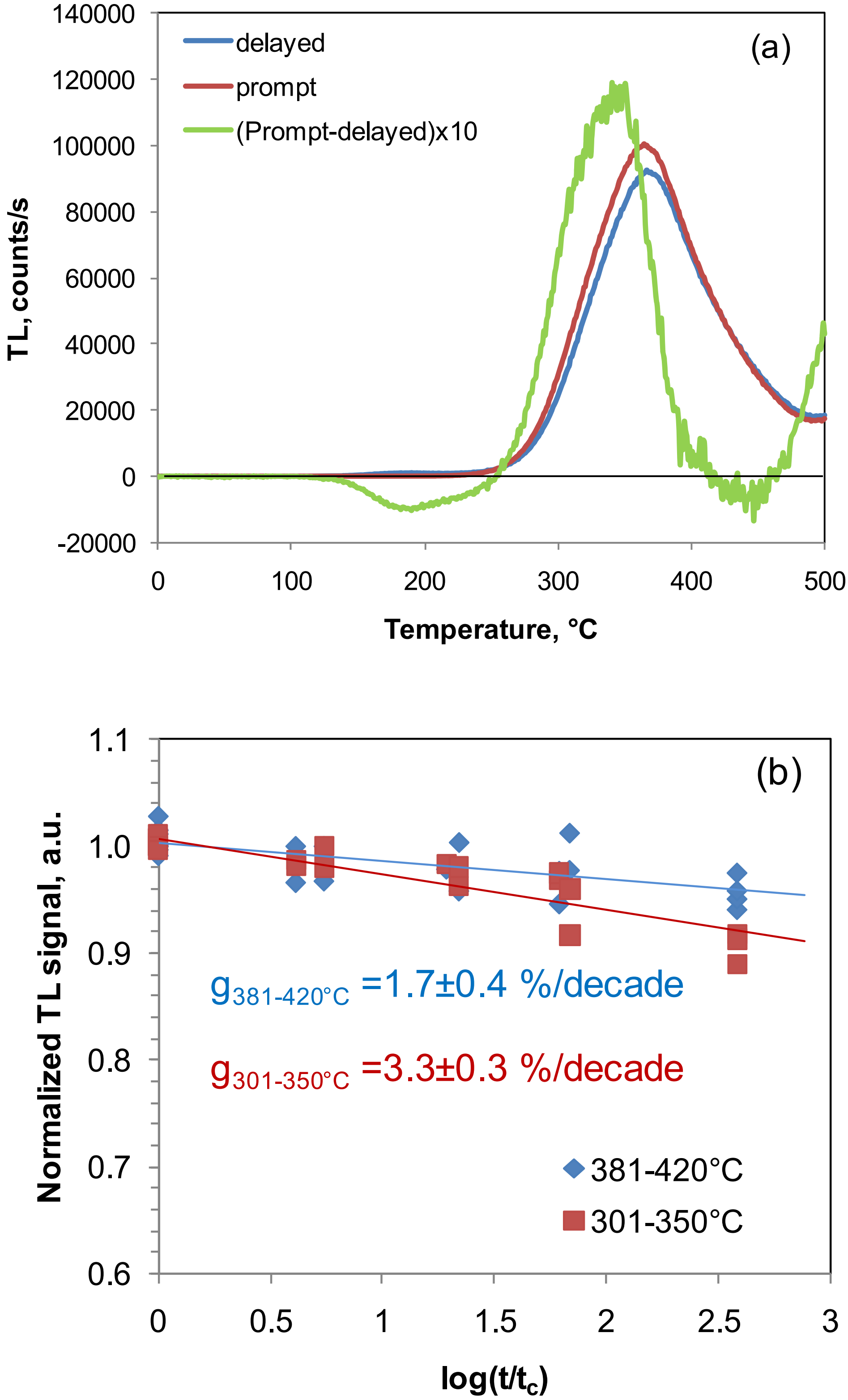
(a)
delayed
prompt
(Prompt-delayed)x10
TL, counts/s
140000
120000
100000
80000
60000
40000
20000
0
-20000
0
100
200
300
400
500
Temperature, °C
(b)
Normalized TL signal, a.u.
1.1
1.0
0.9
0.8
0.7
0.6
g381-420°C =1.7±0.4 %/decade
g301-350°C =3.3±0.3 %/decade
381-420°C
301-350°C
0
0.5
1
1.5
2
2.5
3
log(t/tc)